

Pressure and Temperature Derivatives of the Low-Frequency Dielectric Constants of LiF, NaF, NaCl, NaBr, KCl, and KBr^{†*}

John Fontanella

United States Naval Academy, Annapolis, Maryland 21402

and

Carl Andeen and Donald Schuele

Case Western Reserve University, Cleveland, Ohio 44106

(Received 13 September 1971)

The first-, second-, and third-order 308°K pressure derivatives of the low-frequency dielectric constants for LiF, NaF, NaCl, NaBr, KCl, and KBr have been determined to an accuracy of about 0.2%, 2%, and 20%, respectively. In addition, the first- and second-order temperature derivatives are established at approximately the 0.2% and 20% level. The volume-independent temperature derivative of the low-frequency dielectric constant is found to be negative for LiF and positive for the remaining crystals. This trend may be understood in terms of the interaction between the acoustic and optic modes using Szigeti's formalism for anharmonic crystals as interpreted by Fuchs. The results are also used to show that the question as to the interpretation of the Szigeti effective charge remains open for the alkali halides.

INTRODUCTION

The static dielectric constant ϵ_s and its variation with temperature and pressure contain important information concerning the constitution of solids. The constant itself provides a measure of the ability of polarizable entities within the solid to respond to an electric field. The variation of ϵ_s with pressure, then, reflects how these systems are affected by a change in interatomic distance while the temperature dependence of ϵ_s includes both analogous size effects and those that are intrinsically thermal. An accurate mapping of ϵ_s in the PT plane, then, is of interest and importance in the study of solids.

Until recently, it had been very difficult to obtain an accurate value of the static dielectric constant from the literature. This situation is discussed and many of the problems regarding the measurement of ϵ_s for some common ionic crystals are resolved in previous papers by the authors.¹⁻³

Similarly, past values for the pressure and temperature dependence of the static dielectric constant of solids show an unusual amount of scatter. The results of most of the major work in this area are tabulated in a recent paper by Lowndes and Martin.⁴ The ranges of values listed for $(1/\epsilon_s)(\partial\epsilon_s/\partial p)_T$ for the crystals with which the present work deals are the following: LiF, 3.4-4.87; NaF, 5.06-5.3; NaCl, 9.2-10; NaBr, 11.3-12.39; KCl, 9.92-10.57; and KBr, 9.9-13.4 (units of 10^{-12} cm²/dyn). The temperature derivatives listed there generally show deviations of about 3% with the exception of LiF, where values of 28.2 and 37.3 10^{-5} °K⁻¹ are given.

This paper presents new, more accurate, first-order, temperature and pressure derivatives of the static dielectric constant for the above crystals which are used to recalculate some quantities of fundamental interest. In addition, higher-order derivatives are given which are used to make some new calculations.

EXPERIMENT

Once the static dielectric constant has been established for a particular pressure and temperature, only relative changes in ϵ_s with pressure and temperature need to be determined. Thus, the main limitations¹⁻³ on standard geometrical methods do not apply. Consequently, the usual three-terminal geometrical technique is potentially quite accurate and was chosen for the present work. As pointed out previously¹⁻³ the remaining problems are those associated with the use of contact electrodes and with fringing-field effects.

It has been shown⁵ that air gaps often occur between electrodes and samples and can have significant influence on the accurate measurement of dielectric-relaxation phenomena in alkali halides. For this reason evaporated electrodes were used in this work. Also it has been shown⁶ that capacitance enhancement can result from the interaction of platinum electrodes with alkali halides at high temperatures. This effect was eliminated by using gold as the electrodes and avoiding high temperatures.

For disc-shaped samples as used in this work, fringing fields arise at the gap between the guard ring and guarded electrode and at the edge of the crystal. The former effect was minimized great-

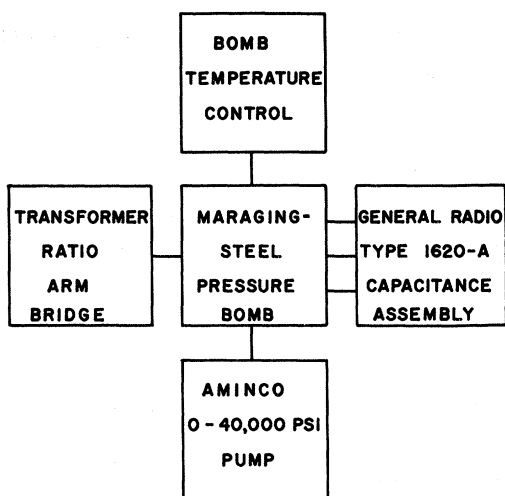


FIG. 1. Block diagram of the apparatus used for the measurement of the room temperature (308°K) pressure derivatives of the static dielectric constant.

ly by achieving extremely small gaps. This was accomplished by first evaporating the guard electrode using a carefully machined mask that covered the center portion of the crystal. Next, the guarded center electrode was evaporated using a washer-type mask whose inside diameter was slightly smaller than the inside diameter of the previously evaporated guard electrode. The centering of the sample was done under a microscope using three screw-type mechanisms. The sample was spring-loaded to allow for isotropic thermal expansion. In this manner it was possible to obtain gaps which were less than 12 μm wide.

The samples (some of those for which the low-frequency dielectric constants are reported in a previous article²) were 25 mm in diameter and 1.6 mm thick. The guarded electrode was 14 mm in diameter, and thus the condition that fringing field effects be eliminated, (guard ring width)/(sample thickness) > 3, is more than satisfied.

All evaporations were done with the sample at 180°C after having been outgassed at that temperature for 1 h. Some of the films were made approximately 2000 Å thick and others 200 Å as a check for possible thin-film stress effects.

A block diagram of the apparatus used to measure the room-temperature (308°K) pressure derivatives of the static dielectric constant is shown in Fig. 1. Three samples at a time were inserted in the Vascomax 300 maraging-steel bomb, a cross section of which is shown in Fig. 2. It is noted that four samples are shown there. The fourth space was occupied by one of the CaF_2 pressure standards described elsewhere.⁷ As explained there, the CaF_2 crystal along with its

associated electronics constitutes a 0.01% pressure gauge. The temperature of the bomb was controlled to within 0.0005°C during the period of a run by means of a feedback temperature controller which used a glass-encapsulated thermistor as the temperature-sensing element. A modified General Radio Type No. 1620-A capacitance measuring assembly, operated at 30 V and 1 kHz, was used to measure the capacitance of the samples to within 1 ppm and is described in Ref. 1-3. The pressure was generated by an Aminco 0-40 000-lb/in.² pump of standard piston-ball-check design, and the pressure fluid used was Simplex projector oil which is a highly refined petroleum oil.

Zero-pressure temperature derivatives of capacitance were measured using the apparatus depicted in the block diagram in Fig. 3. Low temperatures were achieved in a Cryogenics Associates Inc. CT-14 Dewar, and the temperature was controlled using feedback concepts. The sample holder is made of beryllium copper, and is of a design similar to the maraging-steel bomb described above. Temperatures were determined by measuring the resistance of a platinum resistance thermometer using the 27-Hz bridge mentioned in Refs. 2 and 3 and are thought to be accurate to within $\pm 0.1^\circ\text{C}$.

RESULTS

Pressure Derivatives

1. Raw Data

Typical capacitance-vs-pressure data are shown in Fig. 4. The numbers for each pressure run were fitted to a cubic equation of the form

$$C/C_0 = 1 - A_1 p + A_2 p^2 - A_3 p^3, \quad (1)$$

where C_0 is the zero-pressure, 308°K capacitance. The results are listed in Table I with the sample identification as given in a previous paper.² For NaCl and KCl the estimated experimental uncertainties associated with A_1 , A_2 , and A_3 are 0.1%, 1%, and 10%, respectively. The linear term for LiF and NaF is correct to about 0.1% also, but, due to the rather small magnitude of the quadratic and cubic terms, their experimental uncertainties are about 3% and 30%, respectively. Due to the softness and more hygroscopic nature of KBr and NaBr, additional ambiguities place the uncertainty of A_1 , A_2 , and A_3 for these crystals at about 0.2%, 2%, and 20%, respectively. Comments similar to those made for the static dielectric constant related to the effects of random trace impurities^{2,3} can also be made for the pressure derivatives. Even though the static dielectric constants of LiF and NaF from two sources, the Harshaw Chemical Co. and Optovac, Inc., were very uniform, the losses were not, $10^6 \tan \delta$ being

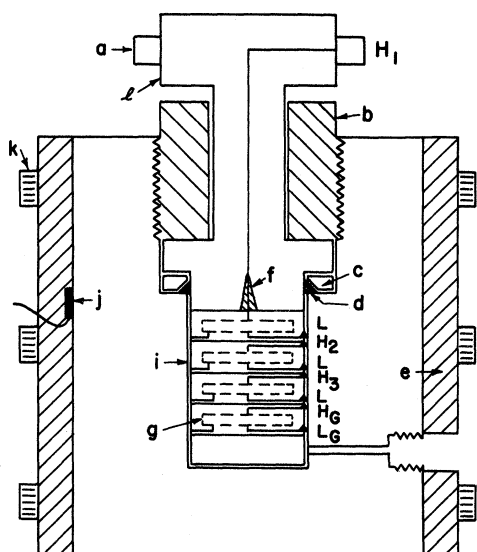


FIG. 2. Maraging-steel bomb and associated parts: (a) BNC connectors; (b) maraging-steel collar; (c) O ring; (d) beryllium-copper armor ring; (e) aluminum jacket; (f) high-pressure electrical lead-through; (g) sample; (i) brass can; (j) glass-encapsulated thermistor; (k) heating resistor; (l) maraging-steel closure plug.

40 and 87 for Harshaw and Optovac LiF, and 45 and 35 for Harshaw and Optovac NaF, respectively. The variation of the pressure derivatives of the static dielectric constant is directly correlated with the trends in the loss for the two materials.

In the case of KCl, the largest pressure derivative occurs for the sample having the greatest value of the static dielectric constant. KCl sam-

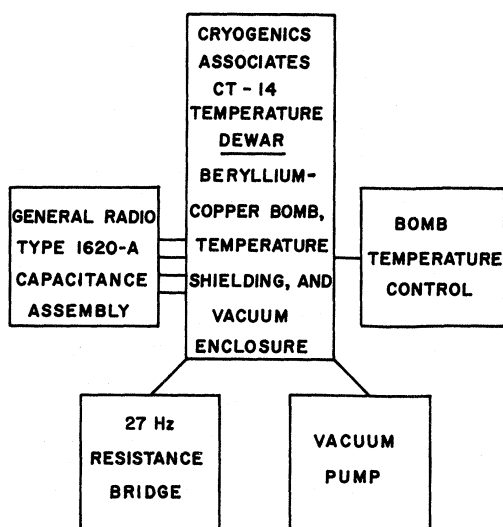


FIG. 3. Block diagram of the apparatus used for the measurement of the zero-pressure temperature derivatives of the static dielectric constant.

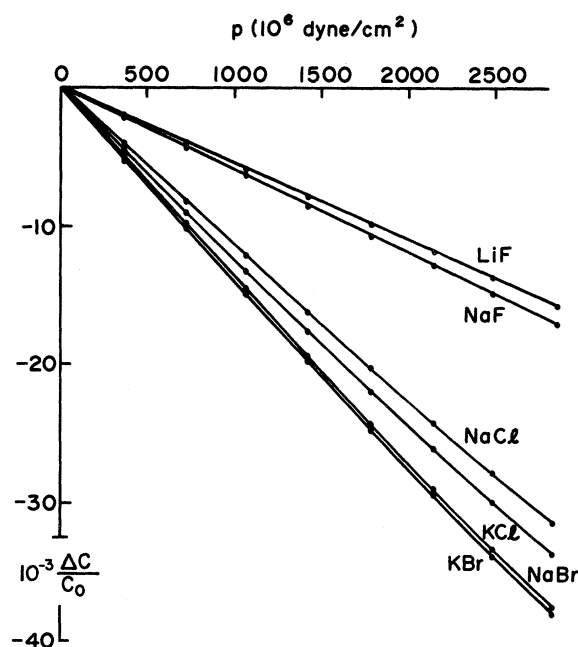


FIG. 4. Plot of pressure vs capacitance change for the alkali halides. The experimental uncertainty is less than the width of the line.

ples XI and III show a corresponding increase of pressure derivative with static dielectric constant, but sample IV does not fit into the scheme. For KBr, the two samples with the largest static dielectric constant also show the largest pressure derivatives. In addition, it is noted that the most uniform values of the pressure derivatives were obtained for NaCl which were correspondingly the most uniform samples taking both the static

TABLE I. Coefficients in the equation $C/C_0 = 1 - A_1 p + A_2 p^2 - A_3 p^3$, where p is in units of dyn/cm^2 .

Identification	300°K ϵ_s	A_1	A_2	A_3
		$(10^{-12} \frac{\text{cm}^2}{\text{dyn}})$	$(10^{-22} \frac{\text{cm}^4}{\text{dyn}^2})$	$(10^{-33} \frac{\text{cm}^6}{\text{dyn}^3})$
LiF	II (H)	9.0357	5.591	0.477
	IV (O)	9.0357	5.603	0.482
NaF	I (H)	5.0722	6.121	0.698
	V (O)	5.0719	6.118	0.677
NaCl	VIII (O)	5.8954	11.802	2.772
	III (H)	5.8952	11.798	2.798
	IX (O)	5.8952	11.798	2.771
	VIII (H)	5.8944	11.791	2.774
NaBr	I (H)	6.3972	14.401	4.190
	III (O)	6.3966	14.424	4.858
KCl	XI (O)	4.8126	12.937	3.887
	IV (H)	4.8115	12.985	4.156
	III (H)	4.8113	12.927	3.939
	VI (O)	4.8179	13.001	4.165
KBr	VII (O)	4.8762	14.776	5.580
	I (H)	4.8738	14.722	5.513
	VIII (O)	4.8758	14.802	5.788

TABLE II. Basic data used in the reduction of room-temperature (308°K) pressure and temperature derivatives.

Quantity	LiF	NaF	NaCl	NaBr	KCl	KBr
χ_T $\left(10^{-12} \frac{\text{cm}^2}{\text{dyn}}\right)$	1.535	2.165	4.230	5.126	5.830	6.836
$(\partial\chi_T/\partial T)_p$ $\left(10^{-15} \frac{\text{cm}^2}{\text{dyn}^\circ\text{K}}\right)$	0.90	1.23	3.05	3.37	4.24	4.63
$(\partial\chi_T/\partial p)_T$ $\left[10^{-24} \left(\frac{\text{cm}^2}{\text{dyn}}\right)^2\right]$	-11.5 ^a	-25.2 ^b	-99.6 ^c	-137.6 ^b	-183.1 ^c	-255.4 ^b
γ_p $(10^{-5}/^\circ\text{K})$	10.35	9.92	12.07	12.75	11.19	11.79
$(\partial\gamma_p/\partial T)_p$ $(10^{-7}/^\circ\text{K}^2)$	1.47	1.23	0.79	0.6	0.57	0.64
$(\partial^2\chi_T/\partial p^2)_T$ $\left[10^{-36} \left(\frac{\text{cm}^2}{\text{dyn}}\right)^3\right]$	170	590	4700	7400	11500	19100
ϵ_s	9.0552	5.0834	5.9094	6.4133	4.8233	4.8856

^aReference 10.^bReference 8.^cR. A. Bartels and D. E. Schuele, J. Phys. Chem. Solids **26**, 537 (1965).

dielectric constant and loss into account.

The effects of electrode thickness on the pressure derivatives were investigated by making the films on NaCl sample VIII about 200 Å thick, while all of the others were approximately 2000 Å thick. The effects are negligible at the level of the current investigation.

The coefficients of capacitance listed in Table I were averaged and the zero-pressure derivatives of the capacitance obtained from

$$\frac{1}{C_0} \left(\frac{\partial C}{\partial p} \right)_T = -\bar{A}_1, \quad (2a)$$

$$\frac{1}{C_0} \left(\frac{\partial^2 C}{\partial p^2} \right)_T = 2\bar{A}_2, \quad (2b)$$

and

$$\frac{1}{C_0} \left(\frac{\partial^3 C}{\partial p^3} \right)_T = -6\bar{A}_3. \quad (2c)$$

2. Data Reduction

The basic data necessary for transforming the pressure derivatives of capacitance to the pressure derivatives of the static dielectric constant are listed in Table II. The isothermal compressibility for each material except LiF is the temperature-corrected average of the values tabulated by Roberts and Smith⁸ and by Leibfried and Ludwig.⁹ The value of χ_T for LiF is a temperature-corrected average of the values given by Miller and Smith¹⁰ and by Leibfried and Ludwig. The

values for the first isothermal pressure derivatives of χ_T are obtained from the references given in Table II. The expression for the second isothermal pressure derivative of χ_T in terms of the isothermal bulk modulus

$$B_T = -v \left(\frac{\partial p}{\partial v} \right)_T = \frac{1}{\chi_T} \quad (3)$$

is

$$\left(\frac{\partial^2 \chi_T}{\partial p^2} \right)_T = \frac{2}{B_T^3} \left(\frac{\partial B_T}{\partial p} \right)_T^2 - \frac{1}{B_T^2} \left(\frac{\partial^2 B_T}{\partial p^2} \right)_T. \quad (4)$$

The quantities on the right-hand side of Eq. (4) have been evaluated for AgBr¹¹ for which it is found that the second term is 10% of the first, and thus the approximation is made that

$$\left(\frac{\partial^2 \chi_T}{\partial p^2} \right)_T \approx \frac{2}{B_T^3} \left(\frac{\partial B_T}{\partial p} \right)_T^2 = \frac{2}{\chi_T} \left(\frac{\partial \chi_T}{\partial p} \right)_T^2, \quad (5)$$

and the results are listed in Table II.

The pressure derivatives of the static dielectric constant which are listed in Table III were calculated using the equations of Appendix A and the averaged coefficients of capacitance, \bar{A}_1 , $2\bar{A}_2$, and $6\bar{A}_3$. If the results for the first pressure derivative are compared with literature values⁴ it is seen that our values are in general more negative than those of most other workers. This is due in part to our use of higher-order terms to describe the variation of ϵ_s with pressure. The first derivative at zero pressure would certainly

TABLE III. Pressure derivatives of the static dielectric constant.

	$\frac{1}{\epsilon_s} \left(\frac{\partial \epsilon_s}{\partial p} \right)_T$	$\frac{1}{\epsilon_s} \left(\frac{\partial^2 \epsilon_s}{\partial p^2} \right)_T$	$\frac{1}{\epsilon_s} \left(\frac{\partial^3 \epsilon_s}{\partial p^3} \right)_T$
	$\left[10^{-12} \frac{\text{cm}^2}{\text{dyn}} \right]$	$\left[10^{-24} \left(\frac{\text{cm}^2}{\text{dyn}} \right)^2 \right]$	$\left[10^{-36} \left(\frac{\text{cm}^2}{\text{dyn}} \right)^3 \right]$
LiF	-5.085	86.6	-1.61
NaF	-5.398	120.8	-2.63
NaCl	-10.388	491.3	-32.2
NaBr	-12.704	812.6	-85.6
KCl	-11.006	691.2	-47.4
KBr	-12.488	978.1	-110

be more negative than for a smoothed linear fit to all of the data. This is a small effect, however, and it is felt that most of the differences are due to factors intrinsic to the experiments themselves such as poorly defined boundary conditions.

Temperature Derivatives

1. Raw Data

Temperature-vs-capacitance data for LiF and NaBr are plotted in Fig. 5. The curves for the remaining materials fit between these bounds. As seen in Fig. 5, data were taken from 80°K to room temperature. The data from 200–308°K lent themselves particularly well to a power-series expansion of the form

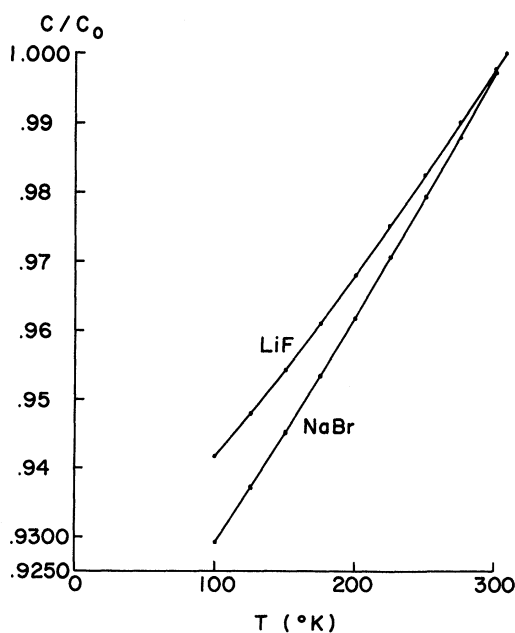


FIG. 5. Plot of temperature versus capacitance change for the alkali halides. The experimental uncertainty is less than the width of the line.

$$C/C_0 = 1 + B_1(T - T_0) + B_2(T - T_0)^2, \quad (6)$$

where $T_0 = 308^\circ\text{K}$ and T is the absolute temperature. It is to be emphasized that this power series has no significance very far beyond the region 200–308°K. The coefficients B_1 and B_2 for each sample are listed in Table IV. The temperature data was fitted only to second order because the accuracy of the temperature values was not sufficient to predict reliable third-order coefficients. The experimental uncertainty is approximately 0.2% for B_1 and about 20% for B_2 . The 308°K temperature derivatives were then obtained from the following equations:

$$\frac{1}{C_0} \left(\frac{\partial C}{\partial T} \right)_{p=0, T=308^\circ\text{K}} = B_1 \quad (7a)$$

and

$$\frac{1}{C_0} \left(\frac{\partial^2 C}{\partial T^2} \right)_{p=0, T=308^\circ\text{K}} = 2B_2. \quad (7b)$$

2. Data Reduction

The data necessary for the transformation of capacitance to static dielectric-constant temperature derivatives are given in Table II. The thermal expansion coefficients and their temperature derivatives were obtained from a graphical analysis of the numbers given by James and Yates,¹² Henglein,¹³ and Yates and Panter.¹⁴

The $p = 0$ 308°K temperature derivatives of the static dielectric constants, which are listed in Table IV, were calculated using the data from Tables II and IV and the equations of Appendix A.

DISCUSSION

In considering the pressure and temperature variation of the static dielectric constant, it is of interest to examine the related volume derivatives rather than the pressure and temperature derivatives themselves. These quantities can be calculated from the thermodynamic relations

TABLE IV. Coefficients in the equation $C/C_0 = 1 + B_1(T - T_0) + B_2(T - T_0)^2$ and the related temperature derivatives of the static dielectric constant.

	Identif-ication	B_1 ($10^{-5}/^\circ\text{K}$)	B_2 [$10^{-7}/(^\circ\text{K})^2$]	$\frac{1}{\epsilon_s} \left(\frac{\partial \epsilon_s}{\partial T} \right)_p$ ($10^{-5}/^\circ\text{K}$)	$\frac{1}{\epsilon_s} \left(\frac{\partial^2 \epsilon_s}{\partial T^2} \right)_p$ [$10^{-7}/(^\circ\text{K})^2$]
LiF	II (H)	30.41	0.79	26.96	0.90
NaF	I (H)	31.56	1.31	28.25	2.00
NaCl	VIII (0) Table II	35.62	1.41	31.59	2.28
NaBr	II (H) I	37.03 37.03	1.43 1.44	32.78	2.38
KCl	IV (H)	33.21	1.60	29.48	2.77
KBr	IV (H)	33.75	1.63	29.82	2.79

TABLE V. Temperature-independent volume derivatives and volume-independent temperature derivatives of the static dielectric constant of the alkali halides.

	$v \left(\frac{\partial \epsilon_s}{\partial v} \right)_T$	$\frac{v}{\epsilon_s} \left(\frac{\partial \epsilon_s}{\partial v} \right)_T$	$\frac{\partial}{\partial p} \left[\frac{v}{\epsilon_s} \left(\frac{\partial \epsilon_s}{\partial v} \right)_T \right]$ (10^{-12} cm ² /dyn)	$v^2 \left(\frac{\partial^2 \epsilon_s}{\partial v^2} \right)_T$	$\left(\frac{\partial \epsilon_s}{\partial T} \right)_v$ ($10^{-5}/^\circ\text{K}$)	$\left(\frac{\partial^2 \epsilon_s}{\partial T^2} \right)_v$ ($10^{-7}/^\circ\text{K}^2$)
LiF	30.0	3.31	-14.7	157	-66.2	(20.7)
NaF	12.7	2.49	-13.3	50	17.8	(15.2)
NaCl	14.5	2.46	-32.8	67	11.5	(39.1)
NaBr	15.9	2.48	-60.5	99	7.6	(51.0)
KCl	9.11	1.89	-38.5	40	40.3	(29.2)
KBr	8.92	1.83	-52.0	44	40.5	(29.6)

$$v \left(\frac{\partial \epsilon_s}{\partial v} \right)_T = - \frac{1}{\chi_T} \left(\frac{\partial \epsilon_s}{\partial p} \right)_T \quad (8)$$

and

$$\left(\frac{\partial \epsilon_s}{\partial T} \right)_v = \left(\frac{\partial \epsilon_s}{\partial T} \right)_p + \frac{\gamma_p}{\chi_T} \left(\frac{\partial \epsilon_s}{\partial p} \right)_T, \quad (9)$$

where χ_T is the isothermal compressibility and γ_p is the volume-thermal-expansion coefficient. The present work also makes it possible to calculate second-order volume derivatives of ϵ_s , the equations for which are derived in Appendix B.

Volume-Dependent Effect

The quantity $v(\partial\epsilon_s/\partial v)_T$ was calculated for each material using Eq. (8) and the results are listed in column 1 of Table V. The quantity $(v/\epsilon_s)(\partial\epsilon_s/\partial v)_T$ is listed in column 2. The columns show that both the total and percentage change in ϵ_s for a given strain decrease with an increase in alkali-ion size and are relatively constant for a group of materials with common alkali ion.

The temperature-independent volume derivatives of ϵ_s can also be used to make more specific comments about the nature of solids. In particular it can be used to discuss a problem which has been pointed out by Barron and Batana.¹⁵ They assert that the temperature-independent volume derivative of the Szigeti effective charge e^* , which is defined by the Szigeti relation¹⁶

$$\epsilon_s - \epsilon_\infty = \left(\frac{\epsilon_\infty + 2}{3} \right)^2 \frac{(e^*)^2 N}{\pi \nu_t^2 \bar{M}}, \quad (10)$$

where ϵ_∞ is the high-frequency dielectric constant, N is the reciprocal of the molecular volume, ν_t is the characteristic transverse-optic-mode frequency, and \bar{M} is the reduced mass of the ions, should be positive. This follows from the usual interpretation of e^* as a measure of ionic distortion and the expectation that the amount of

distortion should increase as the volume is decreased. Taking the temperature-independent volume derivative of the above Szigeti relation, one obtains

$$\frac{v}{e^*} \left(\frac{\partial e^*}{\partial v} \right)_T = - \frac{1}{2\chi_T} \left\{ \frac{1}{(\epsilon_s - \epsilon_\infty)} \times \left[\left(\frac{\partial \epsilon_s}{\partial p} \right)_T - \left(\frac{\partial \epsilon_\infty}{\partial p} \right)_T \right] - \frac{2}{(\epsilon_\infty + 2)} \left(\frac{\partial \epsilon_\infty}{\partial p} \right)_T + \chi_T (2\gamma_{TO} - 1) \right\}, \quad (11)$$

where $\gamma_{TO} = -(\partial \ln \nu_t / \partial \ln v)_T$. All of the quantities on the right-hand side of Eq. (11) are well known except γ_{TO} , which is extremely difficult to measure. Experiments to determine γ_{TO} have been undertaken, however, and the best experimental values to date, which were communicated to us by Ferraro of the Argonne National Laboratory, are tabulated in the first column of Table VI. In the second column is the maximum value which γ_{TO} can have before $(\partial e^*/\partial v)_T$ becomes negative as deduced from Eq. (11) and the data from Tables II, III, and VI. If compressibility and the pressure derivative of the refractive index are assigned an uncertainty of 1% and the high-frequency dielectric constants are considered accurate to about 0.5%, it follows that these cutoff values of γ_{TO} are about 1% accurate. Unfortunately, the uncertainties associated with the values of $(\gamma_{TO})_{\text{expt}}$ are on the order of the differences between $(\gamma_{TO})_{\text{max}}$ and $(\gamma_{TO})_{\text{expt}}$, and thus no conclusions can be drawn with respect to the sign of $(\partial e^*/\partial v)_T$ and hence the interpretation of e^* .

The increased accuracy of the present work makes it possible to comment on second-order volume effects. The first quantity of interest is the pressure variation of $(v/\epsilon_s)(\partial\epsilon_s/\partial v)_T$ which

TABLE VI. Quantities related to the logarithmic volume derivative of the Szigeti effective charge.

	$(\gamma_{TO})_{\text{expt}}^a$	$(\gamma_{TO})_{\text{max}}$	$(10^{-12} \text{ cm}^2/\text{dyn})$	ϵ_∞^c
LiF	2.6	2.71	0.198	1.926
NaF	3.0	2.53	0.272	1.742
NaCl	2.4	2.83	1.170	2.329
NaBr	3.0	2.92	1.571	2.60
KCl	2.9	2.61	1.816	2.173
KBr	2.6	2.73	2.438	2.358

^aJohn R. Ferraro (private communication).

^bK. Vedam and Joseph L. Kirk (private communication) provided values for all crystals except NaBr. The value for NaBr was obtained by assuming that the fractional change in proceeding from NaCl to NaBr is the same as that for KCl to KBr.

^cR. P. Lowndes and D. H. Martin, Proc. Roy. Soc. (London) **308**, 473 (1969).

is given by

$$\frac{\partial}{\partial p} \left[\frac{v}{\epsilon_s} \left(\frac{\partial \epsilon_s}{\partial v} \right) \right]_T = \frac{1}{\chi_T^2 \epsilon_s} \left(\frac{\partial \epsilon_s}{\partial p} \right)_T \left(\frac{\partial \chi_T}{\partial p} \right)_T + \frac{1}{\chi_T \epsilon_s^2} \left(\frac{\partial \epsilon_s}{\partial p} \right)_T^2 - \frac{1}{\chi_T \epsilon_s} \left(\frac{\partial^2 \epsilon_s}{\partial p^2} \right)_T. \quad (12)$$

The values for this quantity are listed in Table V. It is noted that the values are negative, in disagreement with the observations of Lowndes and Martin.⁴ Of more interest is the second volume derivative which was calculated from Eq. (B2) and which is listed in Table V. It is seen that the values of $v^2(\partial^2 \epsilon_s / \partial v^2)_T$ are positive, which indicates that as the volume decreases the dielectric constant becomes increasingly less responsive to volume changes as might be expected.

Volume-Independent Effect

Next, the volume-independent temperature derivatives were calculated using Eq. (9) and the resultant numbers are listed in Table V. The results are interesting in that the value of $(\partial \epsilon_s / \partial T)_v$ for LiF is negative, while this derivative for the other crystals is positive. This result is thought to be definitive in that if the thermal expansion coefficient is assigned an uncertainty of 2%, the compressibility 1%, and the temperature and pressure derivatives of ϵ_s 0.3% each, the maximum value for $(\partial \epsilon_s / \partial T)_v$ for LiF is $-30 \times 10^{-5} \text{ }^\circ\text{K}^{-1}$.

These results may be understood in terms of the formulation of Szigeti¹⁷ for anharmonic crystals as interpreted by Fuchs.¹⁸ Szigeti writes the dipole moment of the crystal up to third order in the normal coordinates Q as

$$M = \alpha_0 Q_0 + \sum_{ij} \beta_{ij} Q_i Q_j + \sum_{ijk} \gamma_{ijk} Q_i Q_j Q_k, \quad (13)$$

where α_0 , β_{ij} , and γ_{ijk} are constants. He writes the lattice potential energy to fourth order with constants b_{ijk} and c_{ijkl} as

$$W = \frac{1}{2} \sum_i \omega_i^2 Q_i^2 + \sum_{ijk} b_{ijk} Q_i Q_j Q_k + \sum_{ijkl} c_{ijkl} Q_i Q_j Q_k Q_l, \quad (14)$$

where $\omega_i/2\pi$ is the frequency of the i th mode.

Writing the Hamiltonian and applying perturbation theory, Szigeti arrived at the equation

$$\epsilon_s - \epsilon_\infty = \frac{4\pi\alpha_0}{v\omega_0^2} + F + G, \quad (15)$$

where

$$F = \frac{8\pi\hbar}{v} \frac{\alpha_0}{\omega_0^2} \sum_i \left(\gamma_{0ii} - \frac{\alpha_0 c_{00ii}}{\omega_0^2} \right) \frac{\bar{n}_i + \frac{1}{2}}{\omega_i}, \quad (16)$$

$$G = \frac{4\pi\hbar}{v} \sum_{ij} \left(\beta_{ij} - \frac{\alpha_0 b_{0ij}}{\omega_0^2} \right)^2 \times \frac{1}{2\omega_i\omega_j} \left(\frac{1 + \bar{n}_i + \bar{n}_j}{\omega_i + \omega_j} + \frac{\bar{n}_i - \bar{n}_j}{\omega_i - \omega_j} \right), \quad (17)$$

and

$$\bar{n}_i = 1 / (e^{(\hbar\omega_i/kT)} - 1). \quad (18)$$

The first term on the right-hand side of Eq. (15) gives the lattice contribution to the ionic dielectric constant in the absence of any anharmonicities. Fuchs then shows that F makes a negative contribution to the temperature coefficient of the dielectric constant and that G makes a positive contribution, with the latter effect arising from the interaction of the acoustic and optic modes. Thus, it is probable that a low value of $(\partial \epsilon_s / \partial T)_v$ is indicative of a small interaction between the acoustic and optic modes. There is, in fact, reason to believe that there would be less interaction between the acoustic and optic modes in LiF than in the other alkali halides studied in this work. This is because the lithium ion is so small that the fluorine-fluorine interactions become quite significant in LiF. Thus, it would be expected that in an acoustic deformation the lithium ion would not be coupled to the fluorine ions to the extent that the cations of the other alkali halides studied here would be coupled to their respective anions. This effect should be greater yet in LiCl and LiBr and experiments to determine the pressure and temperature derivatives of the static dielectric constant of these materials are currently being undertaken. Fuchs goes on to show that

$$\alpha_0/\omega_0^2 \approx (\epsilon_s + 2), \quad (19)$$

which, from Eqs. (15)–(17), implies that the

materials with higher dielectric constants should have lower values of $(\partial\epsilon_s/\partial T)_v$. This is the trend observed in this work as seen in Tables II and V. It would be of interest to have accurate values for the pressure and temperature variation of the low-frequency dielectric constants for the remaining sodium-chloride-structure alkali halides and for NaI and CsF in particular, in that these crystals have dielectric constants between NaBr and LiF. Experiments on these crystals are being undertaken.

Finally, an approximate value for the second temperature derivative with volume held constant was obtained using Eq. (B6) and the data of Tables II-IV. The values are not exact in that the cross derivative $(\partial^2\epsilon_s/\partial p\partial T)$ has been omitted. This term is most likely positive⁴ and thus the values in the last column of Table V should be slightly more positive.

CONCLUSIONS

It appears, then, that the question as to the sign of $(\partial e^*/\partial v)_T$ and hence the interpretation of e^* for the alkali halides is still open. This work has taken us one step closer to the answer by establishing accurate cutoff values for γ_{TO} . Thus, more accurate values of $(\gamma_{TO})_{\text{opt}}$ are required for the answer to this question.

A negative value of $(\partial\epsilon_s/\partial T)_v$ for LiF is reported. This result can be interpreted in terms of the interaction between the acoustic and optic modes. In addition, a correlation between $(\partial\epsilon_s/\partial T)_v$ and ϵ_s is observed which is consistent with the lattice dynamics of Szigeti as interpreted by Fuchs. Further work on medium-high-dielectric-constant materials would provide useful information on this effect.

ACKNOWLEDGMENTS

The authors would like to thank Dr. John R. Ferraro of the Chemistry Division of Argonne National Laboratory for forwarding the most recent experimental values of the transverse-optic-mode Grüneisen parameter. They also wish to thank Dr. K. Vedam and Joseph L. Kirk of the Materials Research Laboratory of the Pennsylvania State University for supplying some unpublished results for the pressure variation of the refractive index. Finally, the authors would like to express their appreciation to the U. S. AEC for its support throughout the duration of this work.

APPENDIX A: RELATIONS OF THE TEMPERATURE AND PRESSURE DERIVATIVES OF THE STATIC DIELECTRIC CONSTANT TO EXPERIMENTAL OBSERVABLES

The fundamental equation is the expression for the capacitance C of a parallel-plate capacitor of area A , plate separation d , and dielectric of

static dielectric constant ϵ_s :

$$C = \epsilon_s A/d \quad . \quad (\text{A1})$$

Differentiating with respect to pressure, we obtain

$$\frac{1}{\epsilon_s} \left(\frac{\partial\epsilon_s}{\partial p} \right)_T = \frac{1}{C} \left(\frac{\partial C}{\partial p} \right)_T + \frac{\chi_T}{3}, \quad (\text{A2a})$$

where

$$\chi_T = - \frac{1}{V} \left(\frac{\partial V}{\partial p} \right)_T \quad (\text{A3a})$$

is the isothermal compressibility and

$$\frac{1}{\epsilon_s} \left(\frac{\partial^2\epsilon_s}{\partial p^2} \right)_T = \frac{1}{C} \left(\frac{\partial^2 C}{\partial p^2} \right)_T + \frac{2\chi_T}{3} \frac{1}{C} \left(\frac{\partial C}{\partial p} \right)_T + \frac{\chi_T^2}{9} + \frac{1}{3} \left(\frac{\partial\chi_T}{\partial p} \right)_T. \quad (\text{A4a})$$

Differentiating with respect to temperature, we obtain

$$\frac{1}{\epsilon_s} \left(\frac{\partial\epsilon_s}{\partial T} \right)_p = \frac{1}{C} \left(\frac{\partial C}{\partial T} \right)_p - \frac{\gamma_p}{3}, \quad (\text{A2b})$$

where

$$\gamma_p = \frac{1}{V} \left(\frac{\partial V}{\partial T} \right)_p \quad (\text{A3b})$$

is the isobaric coefficient of thermal expansion and

$$\frac{1}{\epsilon_s} \left(\frac{\partial^2\epsilon_s}{\partial T^2} \right)_p = \frac{1}{C} \left(\frac{\partial^2 C}{\partial T^2} \right)_p - \frac{2\gamma_p}{3} \frac{1}{C} \left(\frac{\partial C}{\partial T} \right)_p + \frac{\gamma_p^2}{9} - \frac{1}{3} \left(\frac{\partial\gamma_p}{\partial T} \right)_p. \quad (\text{A4b})$$

Finally, we obtain the equation

$$\begin{aligned} \frac{1}{\epsilon_s} \left(\frac{\partial^3\epsilon_s}{\partial p^3} \right)_T &= \frac{1}{C} \left(\frac{\partial^3 C}{\partial p^3} \right)_T + \frac{\chi_T}{C} \left(\frac{\partial^2 C}{\partial p^2} \right)_T \\ &+ \frac{\chi_T^2}{3C} \left(\frac{\partial C}{\partial p} \right)_T + \frac{\chi_T}{3} \left(\frac{\partial\chi_T}{\partial p} \right)_T \\ &+ \frac{1}{C} \left(\frac{\partial\chi_T}{\partial p} \right)_T \left(\frac{\partial C}{\partial p} \right)_T + \frac{\chi_T^3}{27} + \frac{1}{3} \left(\frac{\partial^2\chi_T}{\partial p^2} \right)_T. \quad (\text{A5}) \end{aligned}$$

APPENDIX B: DERIVATION OF THE SECOND-ORDER VOLUME DERIVATIVES OF ϵ_s

The curvature of the temperature-independent volume derivative is derived using the operator equation associated with Eq. (8):

$$\frac{\partial}{\partial v} \Big|_T = - \frac{1}{\chi_T v} \frac{\partial}{\partial p} \Big|_T \quad (\text{B1})$$

and applying it to itself yields

$$\left(\frac{\partial^2\epsilon_s}{\partial v^2} \right)_T = \frac{1}{\chi_T v} \frac{\partial}{\partial p} \Big|_T \left[\frac{1}{\chi_T v} \left(\frac{\partial\epsilon_s}{\partial p} \right)_T \right]$$

$$\begin{aligned}
&= \frac{1}{\chi_T v} \left[-\frac{1}{\chi_T^2 v} \left(\frac{\partial \epsilon_s}{\partial p} \right)_T \left(\frac{\partial \chi_T}{\partial p} \right)_T \right. \\
&\quad \left. - \frac{1}{\chi_T v^2} \left(\frac{\partial \epsilon_s}{\partial p} \right)_T \left(\frac{\partial v}{\partial p} \right)_T + \frac{1}{\chi_T v} \left(\frac{\partial^2 \epsilon_s}{\partial p^2} \right)_T \right] \\
&\quad + \frac{2\gamma_p}{\chi_T} \frac{\partial^2 \epsilon_s}{\partial T \partial p} + \frac{\gamma_p^2}{\chi_T^2} \left(\frac{\partial^2 \epsilon_s}{\partial p^2} \right)_T + \frac{\gamma_p}{\chi_T} \left(\frac{\partial \gamma_p}{\partial p} \right)_T \left(\frac{\partial \epsilon_s}{\partial p} \right)_T \\
&\quad - \frac{\gamma_p^2}{\chi_T^2} \left(\frac{\partial \chi_T}{\partial p} \right)_T \left(\frac{\partial \epsilon_s}{\partial p} \right)_T. \quad (B4)
\end{aligned}$$

$$\begin{aligned}
&= \frac{1}{\chi_T^2 v^2} \left(\frac{\partial^2 \epsilon_s}{\partial p^2} \right)_T - \frac{1}{\chi_T v^2} \left(\frac{\partial \epsilon_s}{\partial p} \right)_T \left[\frac{1}{\chi_T} \left(\frac{\partial \chi_T}{\partial p} \right)_T - 1 \right]. \quad (B2)
\end{aligned}$$

The volume-independent temperature derivative can be derived from the operator equation associated with Eq. (9) which is

$$\frac{\partial}{\partial T} \Big|_v = \frac{\partial}{\partial T} \Big|_p + \frac{\gamma_p}{\chi_T} \frac{\partial}{\partial p} \Big|_T, \quad (B3)$$

from which it is seen that

$$\begin{aligned}
\left(\frac{\partial^2 \epsilon_s}{\partial T^2} \right)_v &= \left[\frac{\partial}{\partial T} \Big|_p + \frac{\gamma_p}{\chi_T} \frac{\partial}{\partial p} \Big|_T \right] \left[\left(\frac{\partial \epsilon_s}{\partial T} \right)_p + \frac{\gamma_p}{\chi_T} \left(\frac{\partial \epsilon_s}{\partial p} \right)_T \right] \\
&= \left(\frac{\partial^2 \epsilon_s}{\partial T^2} \right)_p + \frac{1}{\chi_T} \left(\frac{\partial \gamma_p}{\partial T} \right)_p \left(\frac{\partial \epsilon_s}{\partial p} \right)_T - \frac{\gamma_p}{\chi_T^2} \left(\frac{\partial \epsilon_s}{\partial p} \right)_T \left(\frac{\partial \chi_T}{\partial T} \right)_p
\end{aligned}$$

The pressure derivative of the thermal expansion coefficient is not known experimentally, but may be determined via the thermodynamic relation

$$\left(\frac{\partial \gamma_p}{\partial p} \right)_T = - \left(\frac{\partial \chi_T}{\partial T} \right)_p. \quad (B5)$$

The final expression is then

$$\begin{aligned}
\left(\frac{\partial^2 \epsilon_s}{\partial T^2} \right)_v &= \left(\frac{\partial^2 \epsilon_s}{\partial T^2} \right)_p + \frac{1}{\chi_T} \left(\frac{\partial \gamma_p}{\partial T} \right)_p \left(\frac{\partial \epsilon_s}{\partial p} \right)_T \\
&\quad + \frac{2\gamma_p}{\chi_T} \left(\frac{\partial^2 \epsilon_s}{\partial p \partial T} \right)_T - \frac{2\gamma_p}{\chi_T^2} \left(\frac{\partial \epsilon_s}{\partial p} \right)_T \left(\frac{\partial \chi_T}{\partial T} \right)_p \\
&\quad - \frac{\gamma_p^2}{\chi_T^2} \left(\frac{\partial \chi_T}{\partial p} \right)_T \left(\frac{\partial \epsilon_s}{\partial p} \right)_T + \frac{\gamma_p^2}{\chi_T^2} \left(\frac{\partial^2 \epsilon_s}{\partial p^2} \right)_T. \quad (B6)
\end{aligned}$$

[†]Work supported in part by the U. S. AEC.

*Based on work performed at Case Western Reserve University.

¹C. Andeen, J. Fontanella, and D. E. Schuele, *Rev. Sci. Instr.* **41**, 1573 (1970).

²C. Andeen, C. Fontanella, and D. E. Schuele, *Phys. Rev. B* **2**, 5068 (1970).

³C. Andeen, J. Fontanella, and D. E. Schuele, *J. Appl. Phys.* **42**, 2216 (1971).

⁴R. P. Lowndes and D. H. Martin, *Proc. Roy. Soc. (London)* **A316**, 351 (1970).

⁵D. Miliotis and D. N. Yoon, *J. Phys. Chem. Solids* **30**, 1241 (1969).

⁶D. F. Gibbs and B. W. Jones, *J. Phys. C* **2**, 1392 (1969).

⁷C. Andeen, J. Fontanella, and D. Schuele, *Rev. Sci. Instr.* **42**, 495 (1971).

⁸R. W. Roberts and C. S. Smith, *J. Phys. Chem. Solids* **31**, 619 (1970).

⁹G. Leibfried and W. Ludwig, in *Solid State Physics*, Vol. 12, edited by F. Seitz and D. Turnbull (Academic, New York, 1961) p. 367.

¹⁰R. A. Miller and C. S. Smith, *J. Phys. Chem. Solids* **25**, 1279 (1964).

¹¹K. Loje and D. Schuele, *J. Phys. Chem. Solids* **31**, 2051 (1970).

¹²B. W. James and B. Yates, *Phil. Mag.* **12**, 253 (1965).

¹³F. A. Henglein, *Z. Electrochem.* **31**, 424 (1925).

¹⁴B. Yates and C. H. Panter, *Proc. Phys. Soc.* **80**, 373 (1962).

¹⁵T. H. K. Barron and A. Batana, *Phil. Mag.* **20**, 619 (1969).

¹⁶B. Szigeti, *Trans. Faraday Soc.* **45**, 155 (1949).

¹⁷B. Szigeti, *Proc. Roy. Soc. (London)* **A252**, 217 (1959).

¹⁸R. Fuchs, MIT Laboratory Instruments Technical Report No. 167, 1961 (unpublished).